Metals **2015**, *5*, 2289-2302; doi:10.3390/met5042289

OPEN ACCESS

metals

ISSN 2075-4701

www.mdpi.com/journal/metals/

Article

Corrosion Behavior in 3.5% NaCl Solutions of γ-TiAl Processed by Electron Beam Melting Process

Asiful Hossain Seikh [1], Ashfaq Mohammad [2,*], El-Sayed M. Sherif [1,3,*] and Abdulrahaman Al-Ahmari [1,2]

[1] Centre of Excellence for Research in Engineering Materials, Advanced Manufacturing Institute, King Saud University, Riyadh 11421, Saudi Arabia; E-Mails: aseikh@ksu.edu.sa (A.H.S.); aalhmari@ksu.edu.sa (A.A.-A.)

[2] Princess Fatima Alnijiris's Research Chair for Advanced Manufacturing Technology (FARCAMT), Advanced Manufacturing Institute, King Saud University, Riyadh 11421, Saudi Arabia

[3] Electrochemistry and Corrosion Laboratory, Physical Chemistry Department, National Research Centre, Cairo 12622, Egypt

***** Authors to whom correspondence should be addressed;
E-Mails: mashfaq@ksu.edu.sa (A.M.); esherif@ksu.edu.sa (E.-S.M.S.);
Tel.: +966-1146-97372 (A.M.); +966-53-320-3238 (E.-S.M.S.);
Fax: +966-1146-78657 (A.M.); +966-1146-70199 (E.-S.M.S.).

Academic Editor: Hugo F. Lopez

Received: 19 October 2015 / Accepted: 27 November 2015 / Published: 3 December 2015

Abstract: In this work, the corrosion behavior of γ-TiAl alloy produced by electron beam melting (EBM) process in 3.5% NaCl solution was reported. The study has been performed using potentiodynamic polarization resistance and electrochemical impedance spectroscopy techniques and complemented by scanning electron microscopy investigations. All measurements were carried out after different periods of alloy exposure in the chloride solutions and at different temperatures. The results showed that the EBM produced γ-TiAl alloy has excellent corrosion resistance confirmed by the high values of polarization resistance and the low values of corrosion current and corrosion rate. With increase in immersion time, the corrosion potential moved to a higher positive value with a decrease in corrosion current and corrosion rate, which suggests an improvement in corrosion resistance. On the other hand, the increase of temperature was found to significantly increase the corrosion of the processed γ-TiAl alloy.

Keywords: titanium aluminides; corrosion; electron beam melting; polarization; EIS

1. Introduction

Presently, there has been an increasing demand in the development of intermetallic alloys due to the stringent requirements of using high strength and low weight alloys in the automobile and modern aircraft industries. Gamma titanium aluminides (γ-TiAl) are intermetallic alloys, proposed to be used in advanced aircraft turbines [1–3]. γ-TiAl has better high temperature properties and higher specific strength than the conventional superalloys used in turbine fabrication. In addition, the use of γ-TiAl is preferred in aero-turbine industry because of its other several features. They possess light weight and offer superior creep, oxidation, and burn resistance than other titanium alloys. These alloys also have enhanced strength at elevated temperatures. The incorporation of several alloying elements like Al, Nb, Mo, Cr *etc.* enhance the mechanical properties as well as corrosion resistance properties for titanium based alloys due to the formation of protective oxide layers [4,5]. For that it goes without saying that γ-TiAl should also have a good resistance to the harsh corrosive environment inside the turbine.

γ-TiAl alloys having intermetallic properties demonstrate limited plasticity. Manufacturing highly complex geometries from such a material is a quite challenging exercise. Reports are available on processing these alloys through hot forging [6], machining [7], and powder metallurgy [8] routes. It can be deduced from these reports that, these technologies require multiple pre- and post-processing steps. Added to this is the very high cost. A slightly better route is casting. Nevertheless, casting has its own problems such as poor fluidity, easy cracking at stress concentrated portions [9].

Considering the limitations of conventional manufacturing routes, a need exists to look for other options. Recently, electron beam melting (EBM) was shown to produce parts having high strength from γ-TiAl [1]. Yet, it is not well known, how EBM processing would affect properties such as corrosion resistance of the actual γ-TiAl material. Due to the major application in military aircraft, exposure of these materials to marine environment leads major corrosion problem due to chloride ions presents. To date, there is little data available on the corrosion resistance properties of TiAl alloys. Delgado *et al.* [10] reported the corrosion behavior of γ-TiAl in Ringer's solution. It has been found that γ-TiAl has very good corrosion resistance similar to Ti-6Al-4V. Gurappa [11] has investigated the degradation of Ti-24Al-15Nb alloys under different environmental conditions and reported that a protective oxide layer is formed on its surface in marine and industrial environments.

The present study aims at investigating the corrosion resistance of γ-TiAl alloy that was processed using EBM technique after different exposure periods of time, namely, 0, 1, 4, and 24 h in stagnant aerated 3.5% NaCl solutions. It is known that 3.5% NaCl solution provides a simulated marine environment, which is the most corrosive medium for these alloys. The work was carried out at room temperature using potentiodynamic polarization and electrochemical impedance spectroscopy (EIS) measurements, in addition to the use of laser diffraction and scanning electron microscopy in the characterization of the γ-TiAl alloy.

2. Experimental Procedure

2.1. Production of Ti Aluminide Alloy

γ-TiAl powder with nominal composition of Ti-48Al-2Cr-2Nb (at. %) supplied by Arcam AB (Mölndal, Sweden) was used as feedstock material. The powder particles were found to be in the range 45–180 μm with a mean of around 110 μm. This was measured by the laser diffraction technique as depicted in Figure 1. Moreover, the morphology of the powder particle was more or less spherical with smaller satellite particles adhering to the bigger ones, as can be seen from the SEM image of Figure 2.

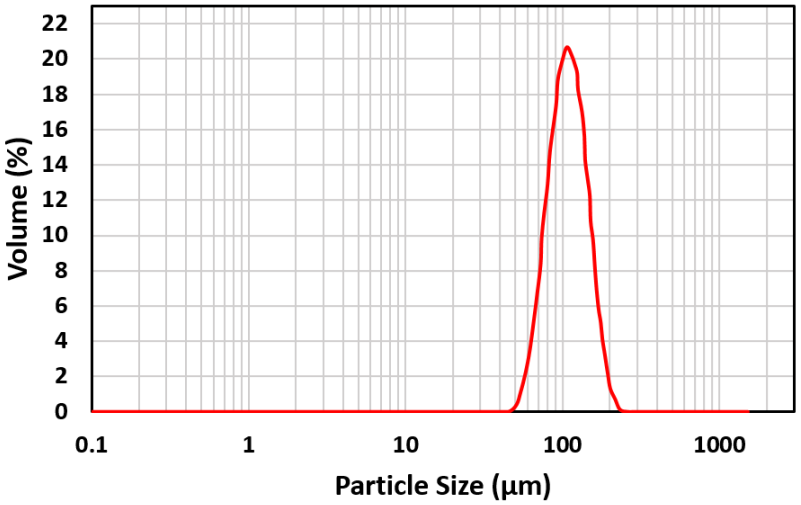

Figure 1. Powder particle size distribution measured by laser diffraction technique.

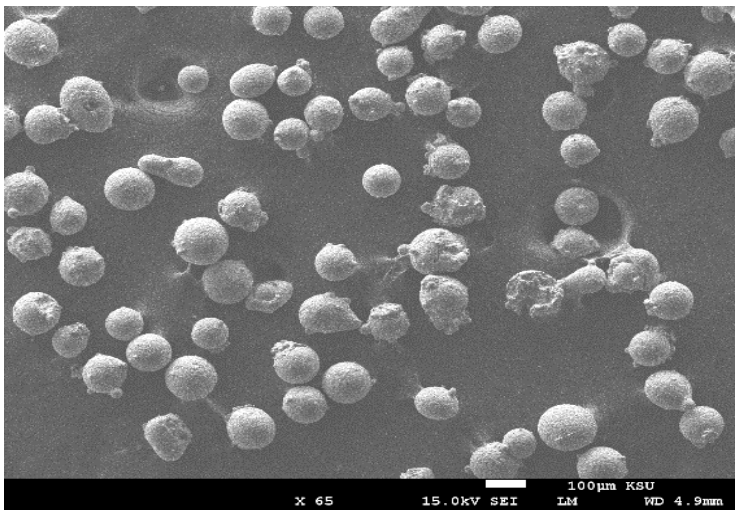

Figure 2. Scanning electron microscopy image of the powder particles before consolidation.

EBM experiments were done on A2 model supplied by ARCAM AB. More details about EBM process setup can be found elsewhere [1]. The specimen dimensions were 25 × 25 × 13 mm height. A 10 mm thick square (100 × 100 mm) stainless steel plate was chosen as the substrate upon which the parts would be built. All the parts after being saved in STL format in Magics (Version 17; Materialise NV, Leuven, Belgium), were then transferred to Build Assembler software (Version 3; Arcam AB, Mölndal, Sweden). This particular software converts the STL geometry into thin slices and writes the

output as machine specific ABF file. The ABF file instructs the machine control on how to proceed with the actual part production.

After the build was completed, the parts were enveloped by the surrounding powder. Because the preheating step envelops the entire area of the substrate plate, the powder around each sample gets slightly sintered. To remove this powder, the build was taken to powder recovery system and blasted with compressed air. To make the blasting more effective, loose powder from the same feedstock was fed along with the air stream.

In EBM the layer thickness was set to 90 microns. Beam current was 25 mA and voltage was set to 60 kV. The beam scan speed was 2400 mm/s. The base plate was heated up to 1050 °C before the first layer of powder was spread on it. Thereafter, the nominal build temperature was set to 1100 °C. The EBM controller maintained the vacuum to about 2×10^{-3} mBar, while the building was continued. The build was surrounded by small amount of helium (He). Ionization of He gave stability of the electron beam and at the same time held down the powder particles thus avoided powder clouding. Powder clouding known as "smoke" can result when electron charge builds up too fast on the surface of the powder particles in the bed. Figure 3 shows SEM image of a surface of the EBM produced γ-TiAl alloy. The corrosion studies were carried out on this same surface. SEM investigations did not reveal any pores of substantial size, suggesting that the consolidation of the powder has been fair enough in the EBM process. The microstructure consisted of laths of γ and α_2 phases. The microstructure was uniform throughout without any clear demarcation of melt tracks. This implies that the adjacent electron beam scans overlapped at an optimum distance and that the subsequent powder layers have fused well.

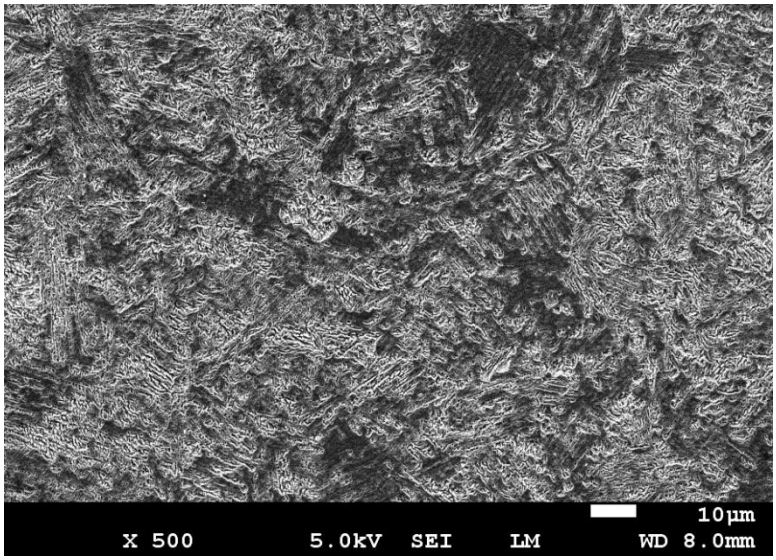

Figure 3. Microstructure of the surface of the fabricated γ-TiAl alloy.

2.2. Chemicals, Materials, and Electrochemical Cell

The electrochemical experiments were performed in a 3.5% NaCl solution with conventional three-electrode cell system in which Ag/AgCl acted as a reference electrode (RE), the platinum foil as a counter electrode (CE) and the produced Ti-Aluminide alloy as the working electrode (WE). The preparation of WE involved a series of steps wherein; a blind hole of about 0.5 mm in depth and diameter was drilled on one surface of the alloy. A long copper wire with similar diameter was placed

in the drilled hole and later soldered to form a rigid joint. The entire assembly was then mounted in an epoxy resin and allowed to cure for 24 h at room temperature. After curing, the other surface was polished using sandpaper of various grit sizes ranging from 180 grit to 1000 grit. The surface was later fine polished using colloidal silica solution to produce a scratch free mirror surface.

2.3. Potentiodynamic Polarization and Electrochemical Impedance (EIS)

The electrochemical experiments were performed using Autolab system manufactured by Metrohm (PGSTAT20, Amsterdam, The Netherlands). The open circuit potential (*versus* Ag/AgCl) was carefully observed after immersing the working electrode in the test solution until the potential stabilized within ±1 mV. Once the potential stability was established, an EIS test was initiated and recorded. The scanning frequency was selected in the range of 100 kHz to 100 MHz, along with an ac wave of ±5 mV peak-to-peak overlaid on a dc bias potential. An equivalent circuit of Nyquist plots was deduced by fit and simulation method. The potentiodynamic polarization curves were obtained by scanning the potential in the forward direction from −0.8 to 0.0 V against Ag/AgCl at a scan rate of 1.67 mV/s. For each experimental condition, three measurements were performed to ensure the reliability and reproducibility of the data.

2.4. Surface Characterization

Scanning electron microscope (SEM) and energy dispersive X-ray (EDX) analyzer both from JEOL (Tokyo, Japan) were employed. The SEM images and the corresponding EDX profile analyses were obtained before and after immersing the alloy in the test chloride solution.

3. Results and Discussion

3.1. Potentiodynamic Polarization Measurements

The corrosion behavior after different periods of exposure in an aerated 3.5% NaCl solution using potentiodynamic polarization measurement of the γ-TiAl alloy, which was produced by electron beam melting (EBM) process, was reported. Figure 4 shows the potentiodynamic polarization curves obtained for the γ-TiAl alloy after (1) 0.0 h; (2) 1.0 h; (3) 4.0 h; and (4) 24 h immersion in 3.5% NaCl solution at room temperature. The corrosion parameters obtained from the polarization curves were calculated and recorded in Table 1. The values of cathodic Tafel (β_c) and anodic Tafel (β_a) slopes, corrosion potential (E_{Corr}), corrosion current density (j_{Corr}) and polarization resistance (R_p) that are listed in Table 1 were obtained as previously reported in our earlier studies [12–14].

Table 1. Potentiodynamic polarization parameters obtained for γ-TiAl alloy in 3.5% NaCl solutions at room temperature.

Exposure Period/h	Parameter				
	β_a/mV dec^{-1}	β_c/mV dec^{-1}	E_{Corr}/mV	j_{Corr}/μA cm^{-2}	R_p/kΩ cm^2
0	65.66	72.81	−497	0.157	255.9
1	62.21	74.95	−538	0.102	339.7
4	60.83	70.75	−591	0.076	368.3
24	65.02	74.34	−595	0.074	440.8

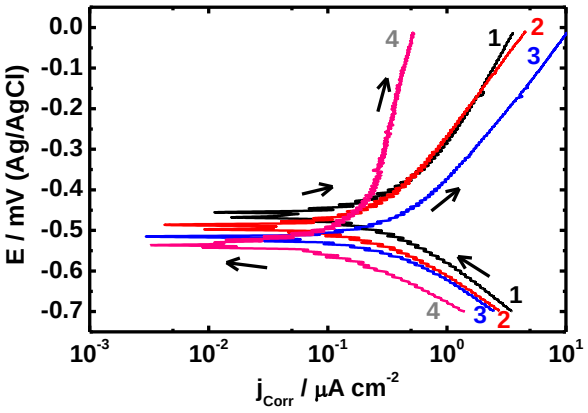

Figure 4. Potentiodynamic polarization curves of γ-TiAl alloy after (**1**) 0.0 h; (**2**) 1.0 h; (**3**) 4.0 h and (**4**) 24 h immersion in 3.5% NaCl solution at room temperature.

It is clearly seen from Figure 4 that the current decreases in the cathodic side reaching the value of j_{Corr}, which is the minimum value of current recorded by the alloy before the current increases again in the anodic branch under the effect of the increase in the applied potential and the aggressiveness influence of chloride ions. It is also seen that the alloy immersed for 0.0 h (curve 1) showed the highest cathodic current, j_{Corr} and the less negative value of E_{Corr}. Increasing the immersion time to 1.0 h (curve 2) decreased the values of cathodic and anodic current and j_{Corr} as well as shifted the value of E_{Corr} towards the more negative direction. Further increases of immersion time to 4.0 h and 24 h decreases the corrosion of the alloy through decreasing its corrosion parameters. This is because the increase of immersion time decreases the uniform attack of γ-TiAl alloy in the chloride solution. This was further confirmed by the parameters that are depicted in Table 1, where the increase of immersion time shifted E_{Corr} to the more negative value and decreased the value of j_{Corr} as well as increased the corrosion resistance values, R_p. The high R_p values correspond to the working electrode opposing any attempt to modify its equilibrium state, resulting in a low rate of titanium ion release and oxide growth. This implies that this alloy has very good corrosion resistance. This behavior was clearly noted for γ-TiAl in Ringer's solution and is in agreement with the results found with potentiodynamic polarization [10].

In order to report the effect of raising temperature on the corrosion of γ-TiAl alloy in the chloride test solution, 3.5% NaCl, potentiodynamic polarization measurements were also carried out. The polarization curves obtained for γ-TiAl alloy in 3.5% NaCl solution at (1) 30 ℃; (2) 40 ℃; (3) 50 ℃; and (4) 60 ℃, respectively are displayed in Figure 5. The values of the corrosion parameters, namely β_c, β_a, E_{Corr}, j_{Corr}, and R_p obtained from the curves shown in Figure 5 are listed in Table 2. The increase of temperature was found to increase the corrosion of the alloy via increasing the cathodic currents, anodic currents and j_{Corr}, while decreased the values of R_p and shifted E_{Corr} to the less negative direction. The corrosion parameters shown in Table 2 proved also that the increase of temperature significantly increases the corrosion of the alloy in the chloride test solution. This is because the increase of temperature increases the activation of the surface of the alloy, which reflects on its fast dissolution and thus the increase of its corrosion [15,16].

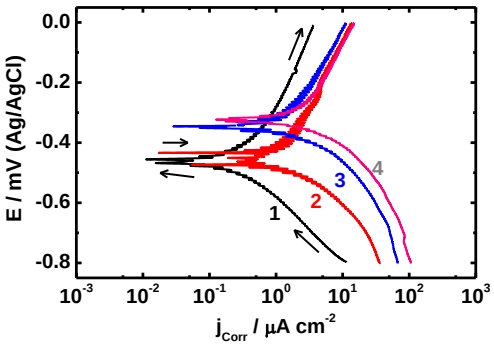

Figure 5. Potentiodynamic polarization behavior for γ-TiAl alloy in 3.5% NaCl solution at (1) 30 ℃; (2) 40 ℃; (3) 50 ℃; and (4) 60 ℃, respectively.

Table 2. Potentiodynamic polarization parameters obtained for γ-TiAl alloy in 3.5% NaCl solutions after different temperatures.

Temperature/ ℃	Parameter				
	β_a/mV dec^{-1}	β_c/mV dec^{-1}	E_{Corr}/mV	j_{Corr}/μA cm^{-2}	R_p/kΩ cm^2
20	65.66	72.81	−497	0.10	255.9
30	66.91	74.74	−438	0.25	166.7
40	60.78	74.09	−356	0.35	105.8
50	61.33	70.82	−330	0.44	70.88
60	64.37	73.85	−322	0.73	50.93

3.2. Electrochemical Impedance Spectroscopy (EIS)

Electrochemical impedance spectroscopy (EIS) method has been normally used to study the corrosion behavior and passivation phenomena for different metals and alloys in a variety of corrosive environments [17–22]. The corrosion behavior of the γ-TiAl alloy samples were carried out in freely aerated stagnant solution of 3.5% NaCl after various immersion periods of time at room temperature and the Nyquist plots obtained at the open-circuit potential are shown in Figure 6. Similar plots were also obtained for the alloy at different temperatures of 20, 30, 40, 50, and 60 ℃ and spectra are shown in Figure 7. The Nyquist plots shown in Figures 6 and 7 were analyzed by fitting the experimental results to an equivalent circuit model shown in Figure 8.

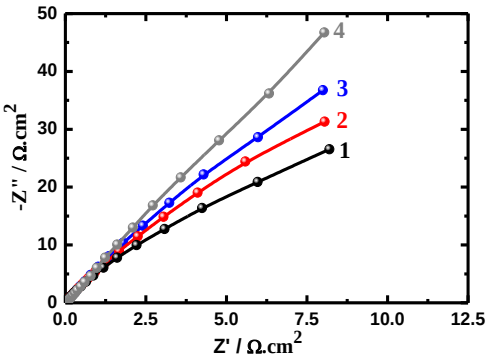

Figure 6. Nyquist plots for γ-TiAl alloy after (1) 0.0 h; (2) 1.0 h; (3) 4.0 h; and (4) 24 h immersion in 3.5% NaCl solution at room temperature.

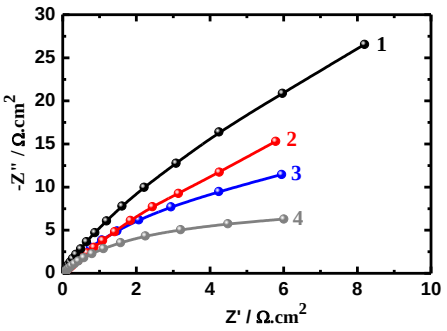

Figure 7. Nyquist plots for γ-TiAl alloy in 3.5% NaCl solution at (1) 30 ℃; (2) 40 ℃; (3) 50 ℃; and (4) 60 ℃, respectively.

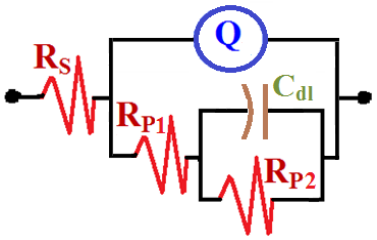

Figure 8. Equivalent circuit model that fits the EIS experimental data.

The elements of the circuit shown in Figure 8 are; the solution resistance (R_S), the constant phase elements (Q) with their n value close to 1.0 refers to a double layer capacitance at the electrode/solution interface (C_{dl}), the polarization resistance (R_{p1}) that can also be defined as the charge transfer resistance at the electrode/solution interface, the double layer capacitance (C_{dl}), and another polarization resistance (R_{p2}) that refers to the resistance of the interface between the corrosion products and the solution. The values of these parameters were determined at room temperature after different immersion periods of time and listed in Table 3. While, the values of the impedance parameters for the γ-TiAl alloy, which were obtained at different temperatures are depicted in Table 4. Among these parameters, R_{p1} and R_{p2} are the factors that determine the corrosion resistance of alloys. This is because the values of R_{p1} and R_{p2} are inversely proportional to j_{Corr}, and hence, high values of R_p correspond to low corrosion rates.

Table 3. EIS parameters obtained for γ-TiAl alloy in 3.5% NaCl solutions at room temperature.

Exposure Period/h	R_S/Ω·cm^2	Q		R_{P1}/Ω·cm^2	C_{dl}/F cm^{-2}	R_{P2}/Ω cm^2
		Y_Q/F cm^{-2}	n			
0	9.22	0.3251	0.73	4.83	0.2992	15.82
1	9.83	0.2978	0.86	6.44	0.2814	21.13
4	9.99	0.2641	0.84	14.2	0.2656	25.35
24	10.03	0.2489	0.89	19.7	0.2115	37.57

Table 4. EIS parameters obtained for γ-TiAl alloy in 3.5% NaCl solutions after different temperatures.

Temperature/ ℃	R_S/Ω cm^2	Q		R_{P1}/Ω cm^2	C_{dl}/F cm^{-2}	R_{P2}/Ω cm^2
		Y_Q/F cm^{-2}	n			
20	9.22	0.325	0.73	4.83	0.2992	15.82
30	8.99	0.338	0.83	4.36	0.3199	12.13
40	8.42	0.345	0.85	3.50	0.3537	9.38
50	8.35	0.383	0.87	2.99	0.3735	7.59
60	8.12	0.394	0.89	2.06	0.4849	5.94

The shapes of Nyquist plots shown in Figure 6 are similar at each exposure period with one depressed semicircle indicating that the corrosion mechanism of the alloy is similar for all regions. It is observed that the diameter of the semicircle remarkably increased with the increase in immersion time, which indicates that the corrosion resistance of the alloy increases with time. The values of R_p listed in Table 3 also increases with the increase of exposure period of time and reveal that the corrosion of the alloy decreases with increasing immersion time. It is also seen that the diameter of the arc, giving the charge-transfer resistance of corrosion reaction, exceeds 100 Ωcm^2. This high R_p value is most probably due to the formation of a stable oxide layer on the γ-TiAl alloy and that has an excellent corrosion resistance in the 3.5 wt. % NaCl solution. It is worth mentioning also that there is a difference between the values of R_{p1} obtained here than those obtained by polarization (Table 1) and this is because polarization is an activation technique, while EIS data are taken at free potential. Moreover, the decrease of the value of the film capacitance (C_{dl}) with increasing immersion time is resulted in turn by the stability of the passive oxide layer formed on the titanium aluminide alloy. Lower values of C_{dl}, especially at long immersion periods of time (Table 3) are corresponding to a slow growth of the oxide film, indicating long-term stability of the passive layer [23,24]. Thus the results from EIS measurements are in good agreement with the obtained polarization data for the γ-TiAl alloy after its immersion for different periods of time in 3.5% NaCl solution.

It is clearly seen from Figure 7 for the γ-TiAl alloy at different temperatures that there is only distorted semicircle at all temperatures, whose diameter gets smaller with increasing the temperature. This indicates that the corrosion of the alloy increases with increasing temperature. This was also confirmed by the values of the EIS parameters shown in Table 4. Where the values of R_{p1} and R_{p2} decreased significantly with temperature and proves that the increase of temperature increases the corrosion for the alloy in the chloride test solution. The value of the constant phase elements (CPEs, Q) with their n values among 0.73 and 0.89 at all temperatures indicate that the CPE represents a double layer capacitor (C_{dl}). This means that the dissolution of the alloy surface is limited by the mass transport, which increases with increasing the solution temperature as was indicated by the increase of C_{dl} value with increasing the temperature. The increased corrosion with temperature can be explained on the basis that the increase of temperature decreases the opportunity for the oxide film formation and thus decreases the corrosion resistance of the surface of γ-TiAl alloy.

The Bode (a) impedance of the interface and (b) the phase angle plots for γ-TiAl alloy after (1) 0.0 h; (2) 1.0 h; (3) 4.0 h; and (4) 24 h immersion in 3.5% NaCl solution at room temperature are shown in Figure 9. It is seen from Figure 9a that the impedance of the interface (|Z|) for the alloy shows lower values, especially at high frequency, increases with decreasing frequency, and the highest values of |Z| are recorded at the lowest frequency values. Increasing the immersion time is obvious to increase the

values of |Z|, which indicates that the increase of immersion time increases the corrosion resistance of the alloy in the chloride solution. This was further confirmed by plotting the change of the degree of phase angle (Φ) with frequency as shown in Figure 9b. It is noted from Figure 9b that the increase of immersion time of the alloy before measurements increases the maximum degree of Φ and that in turn confirms the increase of the passivation of the surface of the aluminum alloy with the increase of time of exposure. However, there is a general trend of the impedance modulus that increases with increasing time of immersion and decreases with increasing temperature, as was also provided by the potentiodynamic results. The EIS data thus confirm the results obtained from the polarization measurements that the increase of immersion time decreases the corrosion of the investigated alloy and that the increase of temperature increases its corrosion.

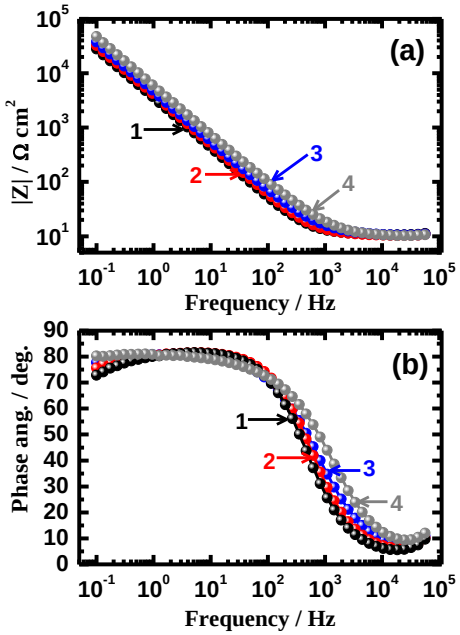

Figure 9. Bode (**a**) impedance of the interface and (**b**) the phase angle plots for γ-TiAl alloy after (1) 0.0 h; (2) 1.0 h; (3) 4.0 h; and (4) 24 h immersion in 3.5% NaCl solution at room temperature.

3.3. Scanning Electron Microscopy (SEM) and Energy Dispersive X-ray (EDX) Analyses

SEM and EDX investigations were carried out on the surface of the γ-TiAl alloy before and after its immersion in the chloride test solution, 3.5% NaCl, in order to report the effect of the chloride solution on the surface of the alloy and to quantify the alloying elements of the alloy before and after corrosion. Figure 10 shows the SEM micrograph and EDX profile analysis for the γ-TiAl alloy before its immersion in 3.5% NaCl solution. The SEM image shows that the surface is clear and homogenous. The EDX corresponding to the SEM image depicted in Figure 10 indicates that the atomic percents for the elements found on the surface of the γ-TiAl alloy were as follows: 46.08% Al, 49.63% Ti, 2.35% Nb, and 1.94% Cr.

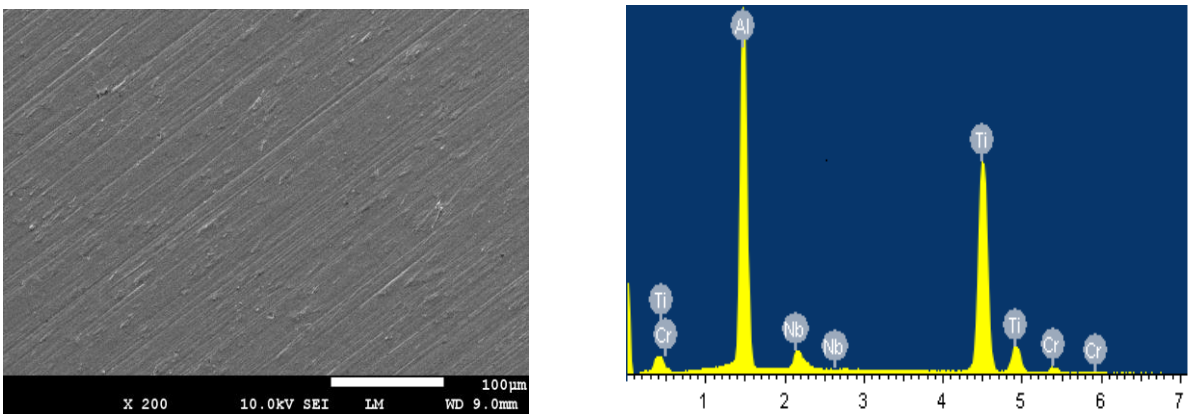

Figure 10. SEM micrograph and EDX profile analysis for the γ-TiAl alloy before its immersion in 3.5% NaCl solution.

The SEM and EDX profile analysis taken after immersing the γ-TiAl alloy for an hour in the chloride solution at room temperature followed by scanning the potential in the forward direction from −0.08 to 0.0 V (Ag/AgCl) are shown in Figure 11. The surface of the alloy is shown to be affected by the severity attack of the chloride ions present in the solution and also the increase of the applied potential towards the positive direction. Here, the SEM image (Figure 11) indicates that the surface is different from the surface shown in Figure 10 from the sample before immersion. Several shallow pits have resulted from immersing the γ-TiAl alloy in 3.5% NaCl solution and from sweeping the potential. The EDX corresponding to the SEM image depicted in Figure 10 indicates that the atomic percents for the elements found on the surface of the γ-TiAl alloy were as following 40.18% Al, 46.69% Ti, 2.25% Nb, 1.65% Cr, and 9.22% O. It is obviously noted from this EDX data that the percent of Al decreased compared to its percent before immersion. This means the corrosion of the alloy might have resulted from the dissolution of Al under the chloride ions attack and the increase of the applied anodic potential. Also, the presence of oxygen is most probably resulting from the formation of aluminum oxide layer on the surface of the alloy, which in turn leads to decreasing the corrosion of the γ-TiAl alloy in 3.5% NaCl solution. The atomic percent for Nb and Cr were almost unchanged before and after immersion, which confirms also that Al is responsible for the corrosion and protection of the alloy.

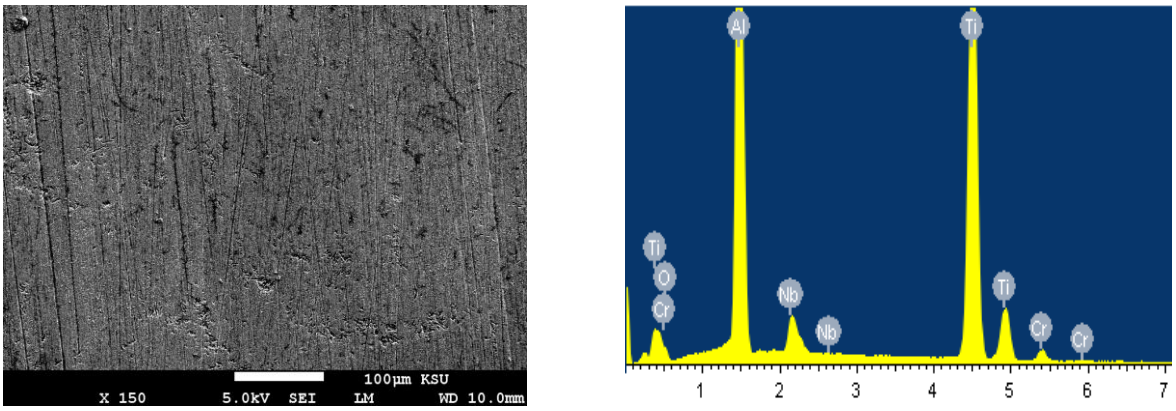

Figure 11. SEM micrograph and EDX profile analysis for the γ-TiAl alloy after its immersion 1 h in 3.5% NaCl solution followed by sweeping the potential from −0.8 V to 0.0 V *vs.* Ag/AgCl.

4. Conclusions

γ-TiAl alloy was produced from metallic powders and processed using electron beam melting (EBM) technique. The corrosion behavior of the produced γ-TiAl alloy was investigated at different temperatures and after different exposure periods of time in 3.5% NaCl solutions. The corrosion tests were carried out using potentiodynamic polarization and EIS techniques. The surface of γ-TiAl alloy was investigated before and after exposure to the chloride solution by using SEM and EDX analyses. The results show that the EBM produced γ-TiAl alloy has excellent corrosion resistance confirmed by the high values of polarization resistance and corrosion potential and low values of corrosion current and corrosion rate. It has been found that the increase in immersion time increases the corrosion resistance of the alloy via decreasing the anodic, cathodic, and corrosion currents and corrosion rate, as well as shifts the corrosion potential towards the positive values. On the other hand, the increase of solution temperature from 20 to 60 ℃ as was indicated by the increase of corrosion parameters is measured by polarization and impedance techniques. SEM/EDX investigations confirmed that the formation of an oxide film on the surface of the alloy is responsible for the corrosion protection of the γ-TiAl alloy, while its corrosion results from the dissolution of aluminum; furthermore, the percentages of Nb and Cr stay almost unchanged before and after the corrosion of the alloy.

Acknowledgments

This project was funded by the National Plan for Science, Technology, and Innovation (MAARIFAH), King Abdulaziz City for Science and Technology, Kingdom of Saudi Arabia, Award Number (11-ADV1494-02).

Author Contributions

A.H. Seikh designed the work and conducted the corrosion experiments. A. Mohammed fabricated the γ-TiAl alloy by EBM and helped in writing the draft of manuscript. E.-S.M. Sherif participated in performing the corrosion tests and wrote the draft manuscript and edited the final manuscript. A. Al-Ahmari helped in manufacturing the alloy and writing the manuscript.

Conflicts of Interest

The authors declare no conflict of interest.

References

1. Murr, L.E.; Gaytan, S.M.; Ceylan, A.; Martinez, E.; Martinez, J.L.; Hernandez, D.H.; Machado, B.I.; Ramirez, D.A.; Medina, F.; Collins, S.; *et al.* Characterization of titanium aluminide alloy components fabricated by additive manufacturing using electron beam melting. *Acta Mater.* **2010**, *58*, 1887–1894.
2. Donachie, M.J., Jr. *Titanium—A Technical Guide*; ASM International: Geauga County, OH, USA, 2000.
3. Wu, X. Review of alloy and process development of TiAl alloys. *Intermetallics* **2006**, *14*, 1114–1122.

4. Draper, L.S.; Das, G.; Locci, I.; Whittenberger, J.D.; Lerch, B.A.; Kestler, H. *Gamma Titanium Alumindes*; Kim, Y.-W., Clemens, H., Rosenberger, A.H., Eds.; TMS: Warrendale, PA, USA, 2003; pp. 207–212.
5. Liu, X.; Chu, P.; Ding, C. Surface modification of titanium, titanium alloys, and related materials for biomedical applications. *Mater. Sci. Eng. R* **2004**, *47*, 49–121.
6. Tetsui, T.; Shindo, K.; Kaji, S.; Kobayashi, S.; Takeyama, M. Fabrication of TiAl components by means of hot forging and machining. *Intermetallics* **2005**, *13*, 971–978.
7. Tetsui, T.; Shindo, K.; Kaji, S.; Kobayashi, S.; Takeyama, M. Strengthening a high-strength TiAl alloy by hot-forging. *Intermetallics* **2003**, *11*, 299–306.
8. Wegmann, G.; Gerling, R.; Schimansky, F.P.; Clemens, H.; Bartels, A. High-temperature mechanical properties of hot isostatically pressed and forged gamma titanium aluminide alloy powder. *Intermetallics* **2002**, *10*, 511–517.
9. Kuang, J.P.; Harding, R.A.; Campbell, J. Microstructures and properties of investment castings of γ-titanium aluminide. *Mater. Sci. Eng. A* **2002**, *329–331*, 31–37.
10. Delgado-Alvarado, C.; Sundaram, P.A. Corrosion evaluation of Ti-48Al-2Cr-2Nb (at. %) in Ringer's solution. *Acta Biomater.* **2006**, *2*, 701–708.
11. Gurrapa, I. Degradation of Ti-24Al-15Nb alloys under different environmental conditions. *Intermetallics* **2003**, *11*, 867–871.
12. Sherif, E.-S.M.; Almajid, A.A.; Latif, F.H.; Junaedi, H. Effects of Graphite on the Corrosion Behavior of Aluminum-Graphite Composite in Sodium Chloride Solutions. *Int. J. Electrochem. Sci*. **2011**, *6*, 1085–1099.
13. Latief, F.H.; Sherif, E.-S.M.; Almajid, A.A.; Junaedi, H. Fabrication of exfoliated graphite nanoplatelets-reinforced aluminum composites and evaluating their mechanical properties and corrosion behavior. *J. Anal. Appl. Pyrolysis* **2011**, *92*, 485–492.
14. Sherif, E.-S.M. Corrosion and Corrosion Inhibition of Aluminum in Arabian Gulf Seawater and Sodium Chloride Solutions by 3-Amino-5-Mercapto-1,2,4-Triazole. *Int. J. Electrochem. Sci.* **2011**, *6*, 1479–1492.
15. Latief, F.H.; Sherif, E.-S.M.; Kakehi, K. Role of Aluminide Coating on Oxidation Resistance of Ni-Based Single Crystal Superalloy at 900 °C. *Int. J. Electrochem. Sci.* **2015**, *10*, 1873–1882.
16. Zubaidy, E.A.H.A.; Mohammad, F.S.; Bassioni, G. Effect of pH, Salinity and Temperature on Aluminum Cookware Leaching during Food Preparation. *Int. J. Electrochem. Sci.* **2011**, *6*, 6424–6441.
17. Darowicki, K.; Krakowiak, S.; Ślepski, P. Evaluation of pitting corrosion by means of dynamic electrochemical impedance spectroscopy. *Electrochim. Acta* **2004**, *49*, 2909–2918.
18. Floyd, F.L.; Avudaiappan, S.; Gibson, J.; Mehta, B.; Smith, P.; Provder, T.; Escarsega, J. Using electrochemical impedance spectroscopy to predict the corrosion resistance of unexposed coated metal panels. *Prog. Org. Coatings* **2009**, *66*, 8–34.
19. Sherif, E.-S.M. Electrochemical investigations on the corrosion inhibition of aluminum by 3-amino-1,2,4-triazole-5-thiol in naturally aerated stagnant seawater. *J. Ind. Eng. Chem.* **2013**, *19*, 1884–1889.
20. Sherif, E.-S.M.; Abdo, H.S.; Khalil, K.A.; Nabawy, A.M. Corrosion Properties in Sodium Chloride Solutions of Al-TiC Composites *in situ* Synthesized by HFIHF. *Metals* **2015**, *5*, 1799–1811.

21. Shinde, V.; Patil, P.P. Evaluation of corrosion protection performance of poly (*o*-ethyl aniline) coated copper by electrochemical impedance spectroscopy. *Mater. Sci. Eng. B* **2010**, *168*, 142–150.
22. Gao, W.; Cao, S.; Yang, Y.; Wang, H.; Li, J.; Jiang, Y. Electrochemical impedance spectroscopy investigation on indium tin oxide films under cathodic polarization in NaOH solution. *Thin Solid Films* **2012**, *520*, 6916–6921.
23. Mansfeld, F.; Fernandes, J.C.S. Impedance spectra for aluminum 7075 during the early stages of immersion in sodium chloride. *Corros. Sci.* **1993**, *34*, 2105–2108.
24. Mansfeld, F.; Han, L.T.; Lee, C.C.; Chen, C.; Zhang, G.; Xiao, H. Analysis of electrochemical impedance and noise data for polymer coated metals. *Corros. Sci.* **1997**, *39*, 255–279.